

**WRINKLE RIDGES ON MERCURY AND THE MOON: A MORPHOMETRIC COMPARISON OF LENGTH-RELIEF RELATIONS WITH IMPLICATIONS FOR TECTONIC EVOLUTION.** Lisa S. Walsh<sup>1,2</sup>, Thomas R. Watters<sup>1</sup>, Maria E. Banks<sup>1</sup>, and Sean C. Solomon<sup>3</sup>. <sup>1</sup>Department of Geology, The University of Maryland, College Park, MD 20742 (lsschlei@umd.edu); <sup>2</sup>Center for Earth and Planetary Studies, National Air and Space Museum, Smithsonian Institution, Washington, DC 20560; <sup>3</sup>Lamont-Doherty Earth Observatory, Columbia University, Palisades, NY 10964.

**Introduction:** On 18 March 2011 the MErcury Surface, Space ENvironment, GEochemistry, and Ranging (MESSENGER) spacecraft transitioned from orbiting the Sun to become the first spacecraft to orbit Mercury. In parallel, the Lunar Reconnaissance Orbiter (LRO) has been orbiting the Moon since 2009, compiling a database of high-resolution images and altimetry of the lunar surface. MESSENGER's orbital phase has returned new images and altimetry of Mercury's northern hemisphere, where broad expanses of smooth plains material have been deformed by wrinkle ridges, contractional tectonic features formed by thrust faulting and folding [1–4]. Data from MESSENGER's flybys and orbital phase, together with earlier observations of Mercury by the Mariner 10 spacecraft, now provide a near-global look at the planet, indicating that smooth plains cover about 27% of Mercury's surface [3, 5–8]. High-incidence-angle (55–75°) images returned during MESSENGER's and LRO's orbital phases enable us to produce more comprehensive global tectonic maps. High-resolution images and altimetric data from MESSENGER and LRO offer an unprecedented opportunity to compare quantitatively the morphology of newly detected wrinkle ridges on Mercury with previously identified wrinkle ridges on the Moon [6, 9–11]. We use these datasets to characterize the length–relief relationships that in part define the morphology of wrinkle ridges on the Moon and Mercury [1, 2, 11–13].

**Length–relief measurements:** We measured the maximum relief and length of 300 wrinkle ridges ( $n = 150$  each for Mercury and the Moon). For Mercury, we measured wrinkle ridges in the northern smooth plains and the Caloris basin interior and exterior plains. For the Moon, we measured wrinkle ridges in all of the major mare basins, including Serenitatis, Crisium, Imbrium, Frigoris, and Oceanus Procellarum. We also examined topographic profiles across wrinkle ridges in (1) Maria Fecunditatis, Tranquillitatis, Nubium, Orientale, Humorum, Cognitum, Nectaris, and Smythii; (2) craters Vitello, Kugler, Karrer, and Grimaldi, and (3) wrinkle-ridge–lobate-scarp transitions. Wrinkle ridges influenced by the presence of buried (ghost) craters [4, 14–15] were not included in the analysis.

Wrinkle ridges were identified on Mercury from a 250-m/pixel mosaic of high-incidence-angle and monochrome images obtained by the Mercury Dual Imaging System (MDIS) on the MESSENGER spacecraft [16]. Mare ridges were characterized from a

100-m/pixel wide-angle camera (WAC) mosaic from the Lunar Reconnaissance Orbiter Camera (LROC) [17]. We used data from the Mercury Laser Altimeter (MLA) ( $n = 49$ ) and the Lunar Orbiter Laser Altimeter (LOLA) ( $n = 39$ ) to measure the maximum relief of wrinkle ridges on Mercury and the Moon, respectively. Relief was measured where the altimeter tracks traverse the wrinkle ridges at angles nearly orthogonal (60° to 90°) to the strike of the ridge [18–19]. The relief was measured directly from MLA and LOLA altimetry tracks where data were available because altimeter tracks provide the densest and most accurate elevation profiles across features and allow detailed viewing of the major morphologic elements of the wrinkle ridge (i.e., the broad arch and superimposed ridge).

Where altimetry tracks were not available, we extracted elevation profiles perpendicular to the structure from gridded digital elevation models (DEMs). For wrinkle ridges in Mercury's northern smooth plains (north of ~40°N), we used a ~500 m/pixel DEM derived by interpolating elevation points from MLA tracks ( $n = 46$ ). For wrinkle ridges south of ~40°N in the Caloris interior and exterior smooth plains, where MLA data points are widely spaced, we measured the relief from DEMs derived from stereo photogrammetry of MESSENGER orbital or flyby images with spatial resolutions from 500 m/pixel to ~2.7 km/pixel ( $n = 55$ ) [20–22]. We measured the relief across north–south-trending wrinkle ridges on the Moon by extracting elevations from a global 100 m/pixel DEM derived from stereo photogrammetric analysis of WAC images ( $n = 111$ ) [23].

**Statistical comparison:** Relief across the wrinkle ridges measured on Mercury ranges from ~112 to 961 m (mean = 404 m,  $n = 150$ ), and the lengths of these wrinkle ridges range from ~27 to 362 km (mean = 94 km). Wrinkle ridges on the Moon range in relief from ~33 to 590 m (mean = 187 m,  $n = 150$ ) and in length from ~10 to 241 km (mean = 53 km). The mean relief of wrinkle ridges on Mercury is ~2.2 times greater than that of wrinkle ridges on the Moon. The mean length of wrinkle ridges measured on Mercury is ~1.8 times greater than the mean length of wrinkle ridges measured on the Moon (Figs. 1 and 2).

**Summary and conclusions:** The majority of wrinkle ridges on Mercury and the Moon are similar in length and relief. The relief–length aspect ratio indicates a similar scaling of length and relief. However, approximately 35% of wrinkle ridges

measured on Mercury are at least 1.8 times longer and ~64% are 2.2 times higher than the largest wrinkle ridges on the Moon. We suggest that these differences in wrinkle ridge length and relief are generated by a combination of differences in (1) thickness of plains material as a control on the maximum depth of faulting, (2) the contribution of subsidence generated by load-induced flexure of the lithosphere, and (3) global contraction due to interior cooling. Global contraction on Mercury is estimated to be at least an order of magnitude larger than on the Moon [13, 25, 26]. Therefore, wrinkle ridges on Mercury that exceed ~600 m in relief are most likely the result of a combination of subsidence and horizontal contraction that accompanied cooling and contraction of the planet's interior, whereas lunar wrinkle ridges formed primarily by subsidence and local thermal contraction of the mare basalt deposits [3, 12, 24].

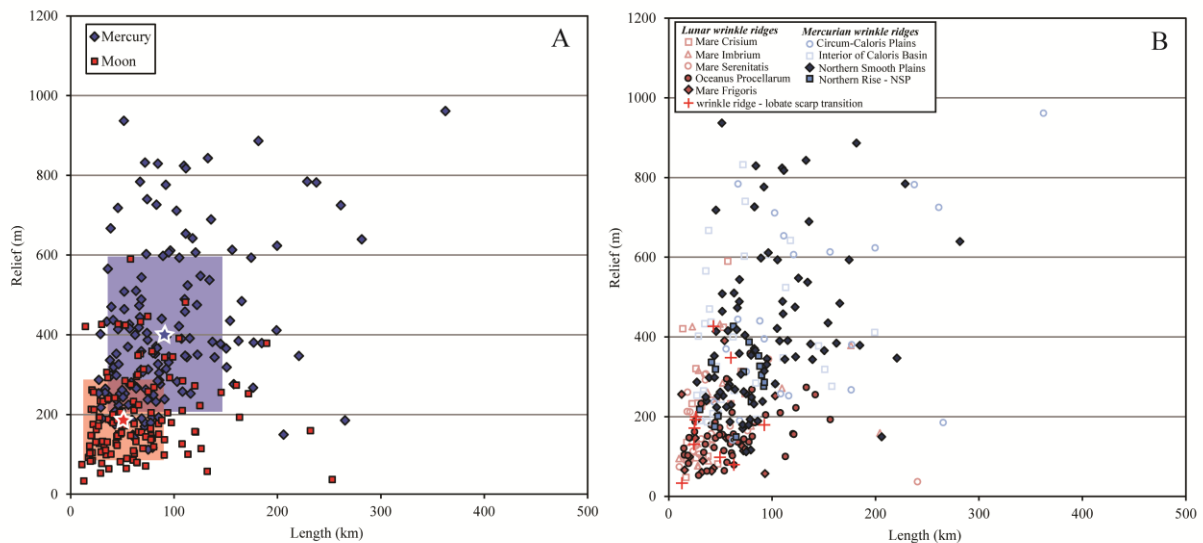


**Figure 1.** (A) Relief versus length for 300 wrinkle ridges on Mercury and the Moon. Wrinkle ridges on Mercury are ~2.2 times greater in mean relief and ~1.8 times greater in mean length than wrinkle ridges on the Moon (stars). The colored rectangles mark the extent of  $\pm$  one standard deviation from the mean relief and length for Mercury (blue) and the Moon (red). (B) Wrinkle ridge dimensions on Mercury and the Moon subdivided by location.

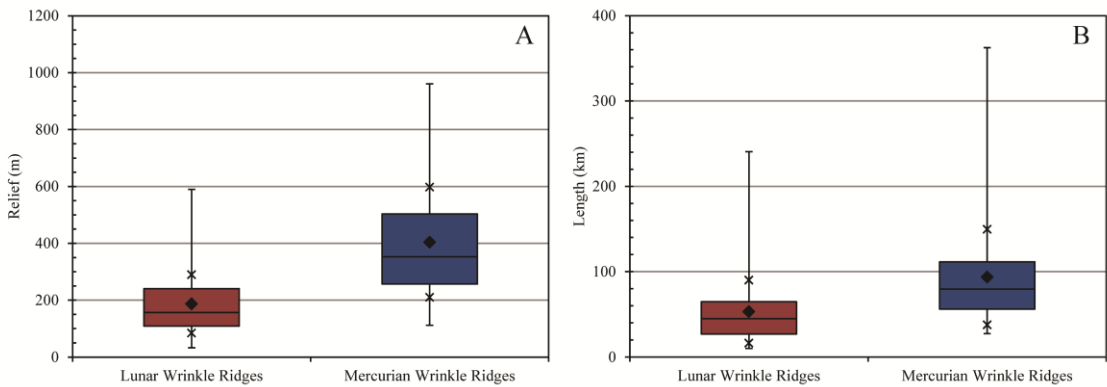


**Figure 2.** Maximum and minimum (A) relief and (B) length of wrinkle ridges on the Moon and Mercury. Mean values are shown as diamonds, median values as horizontal lines, and  $\pm$  one standard deviations as X symbols. The vertical ends of the boxes represent the 2<sup>nd</sup> and 3<sup>rd</sup> quartiles in the distribution values.

- References:** [1] Watters T.R. and Nimmo F. (2010) in *Planetary Tectonics*, Cambridge Univ. Press, pp. 15-80. [2] Watters T.R. and Schultz R.A. (2010) in *Planetary Tectonics*, Cambridge Univ. Press, pp. 209-241. [3] Watters T.R. et al. (2009) *Earth Planet. Sci. Lett.*, 285, 283–296. [4] Head J.W. et al. (2011) *Science*, 333, 1853-1856. [5] Denevi B.W. et al. (2009) *Science*, 324, 613-618. [6] Solomon S.C. et al. (2008) *Science*, 321, 59-62. [7] McNutt R.L., Jr., et al. (2010) *Acta Astronautica*, 67, 681-687. [8] Denevi B.W. et al. (2012) *JGR*, submitted. [9] Strom R.G. (1970) *Eos Trans. AGU*, 51, 773. [10] Maxwell T.A. et al. (1975) *Bull. GSA*, 86, 1273-1278. [11] Watters T.R. (1988) *JGR*, 93, 10239-10254. [12] Strom R.G. et al. (1975) *JGR*, 80, 2478-2507. [13] Watters T.R. et al. (2010) *Science*, 239, 936-940. [14] Klimczak C. et al. (2012) *JGR*, 117, E00L03. [15] Watters T.R. et al. (2012) *Geology*, 40, 1123-1126. [16] Hawkins S.E., III, et al. (2007) *Space Sci. Rev.*, 131, 247-338. [17] Robinson M.S. et al. (2010) *Space Sci. Rev.*, 150, 81-124. [18] Smith D.E. et al. (2010) *Space Sci. Rev.*, 150, 209-241. [19] Zuber M.T. et al. (2012) *Science*, 336, 217-220. [20] Oberst J. et al. (2010) *Icarus*, 209, 230-238. [21] Preusker F. et al. (2011) *Planet. Space Sci.*, 59, 1910-1917. [22] Becker K.J. et al. (2012) *Lunar Planet. Sci.*, 43, 2654. [23] Scholten F. et al. (2012) *JGR*, 117, E00H17. [24] Watters T.R. et al. (2013) *Lunar Planet. Sci.*, 44, this mtg. [25] Solomon S.C. and Head J.W. (1979) *JGR*, 84, 1667-1682. [26] Banks M.E. et al. (2012) *JGR*, 117, E00H11.